Electronic Supplementary Material (ESI) for New Journal of Chemistry.

Supporting Information

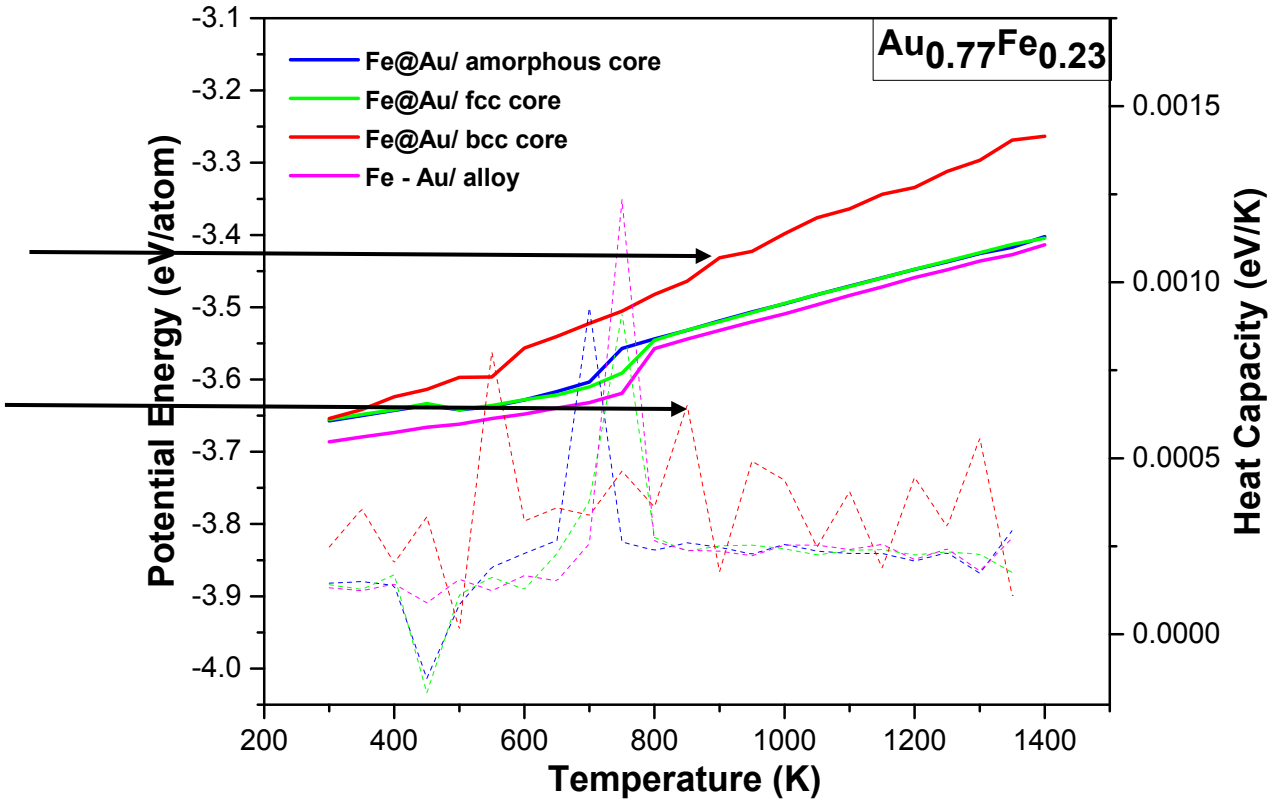

Figure S1. Potential energy (solid lines) and specific heat capacity (dashed lines) of four types of $Au_{0.77}Fe_{0.23}$ bimetallic nanoclusters as a function of temperature.

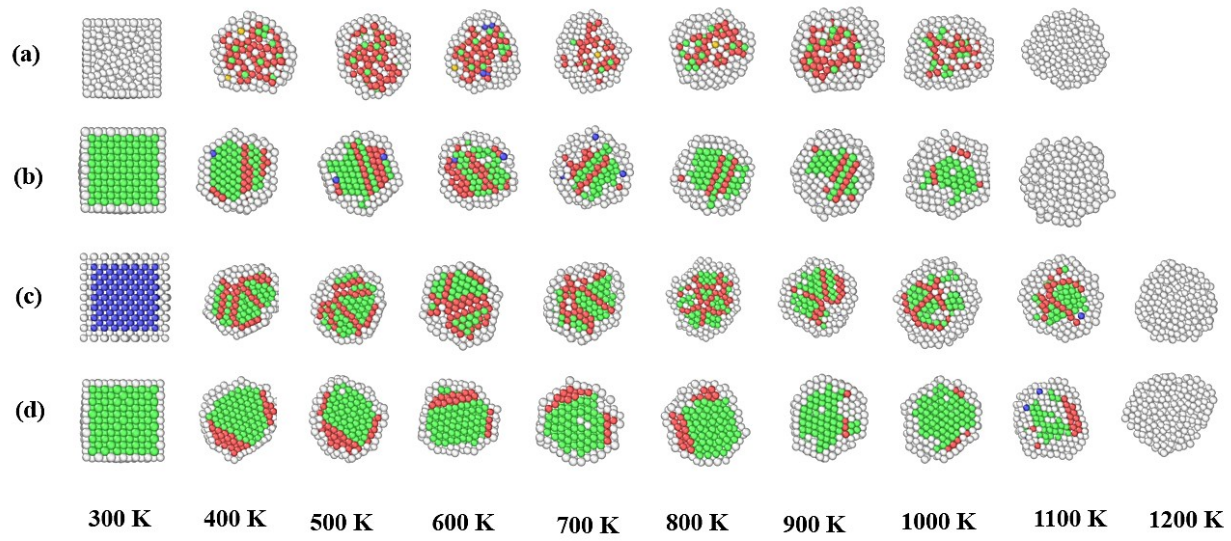

Figure S2. Snapshots of cross sections of distribution of fcc, hcp, bcc, and other atoms in $Au_{0.23}Fe_{0.77}$ NPs including (a) Fe@Au NP with amorphous-core, (b) Fe@Au NP with fcc-core, (c) Fe@Au NP with bcc-core, and (d) Au-Fe nanoalloy NP at different representative temperatures during the heating process. Coloring denotes type of atom: red, hcp atom; green, fcc atom; blue, bcc atom; and light grey, other atom.

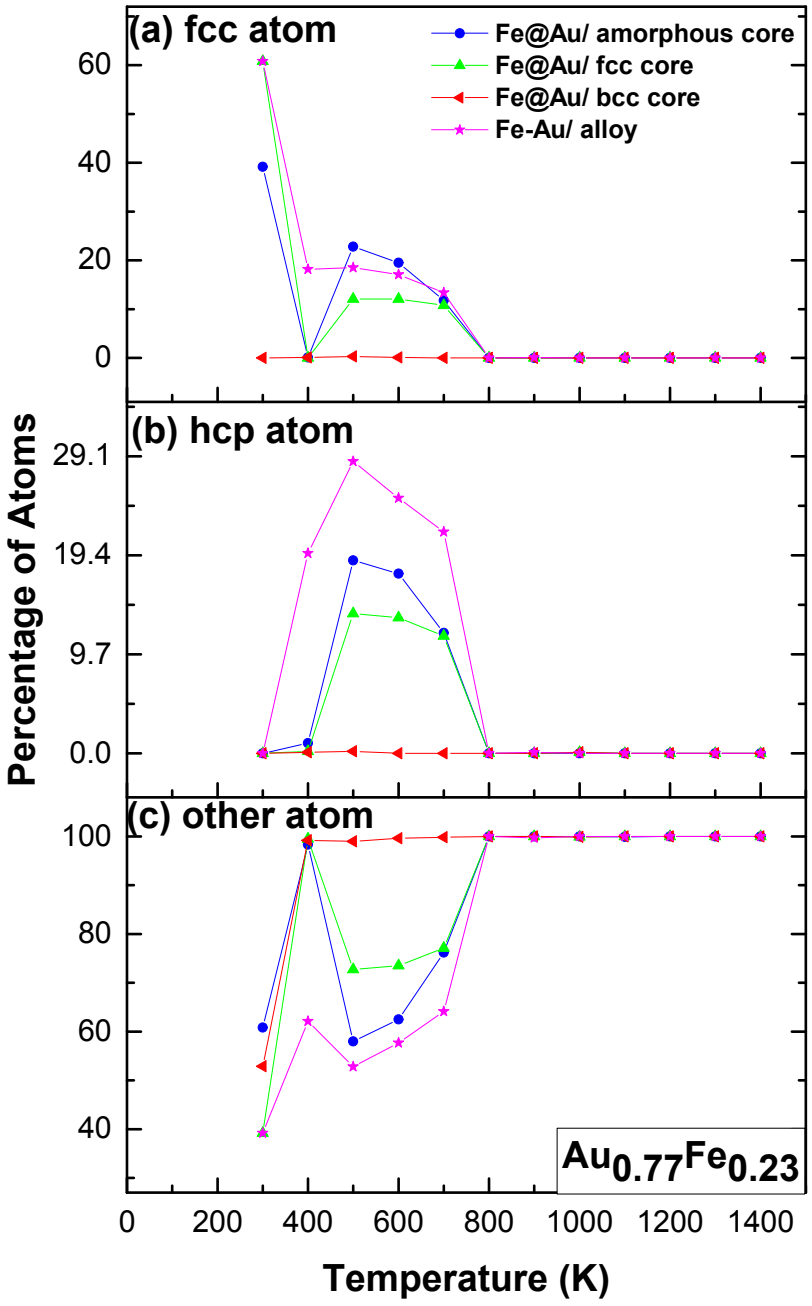

Figure S3. Temperature-dependent percentage of fcc, hcp, and other atoms for four types of $Au_{0.77}Fe_{0.23}$ bimetallic nanoclusters.

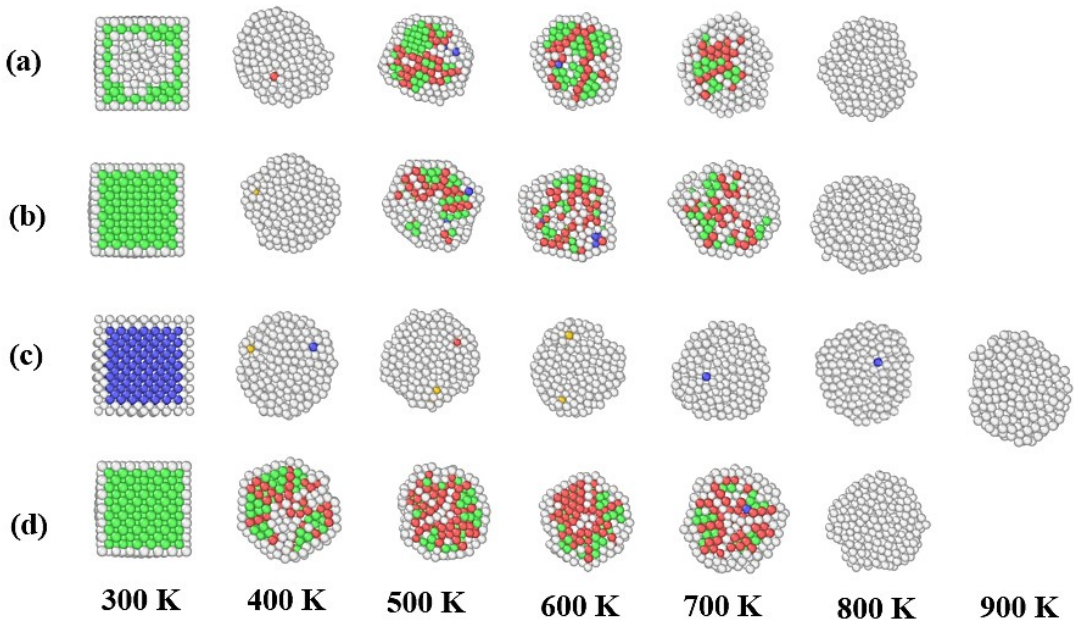

Figure S4. Snapshots of cross sections of distribution of fcc, hcp, bcc, and other atoms in $Au_{0.77}Fe_{0.23}$ NPs including (a) Fe@Au NP with amorphous-core, (b) Fe@Au NP with fcc-core, (c) Fe@Au NP with bcc-core, and (d) Au-Fe nanoalloy NP at different representative temperatures during the heating process. Coloring denotes type of atom: red, hcp atom; green, fcc atom; blue, bcc atom; and light grey, other atom.

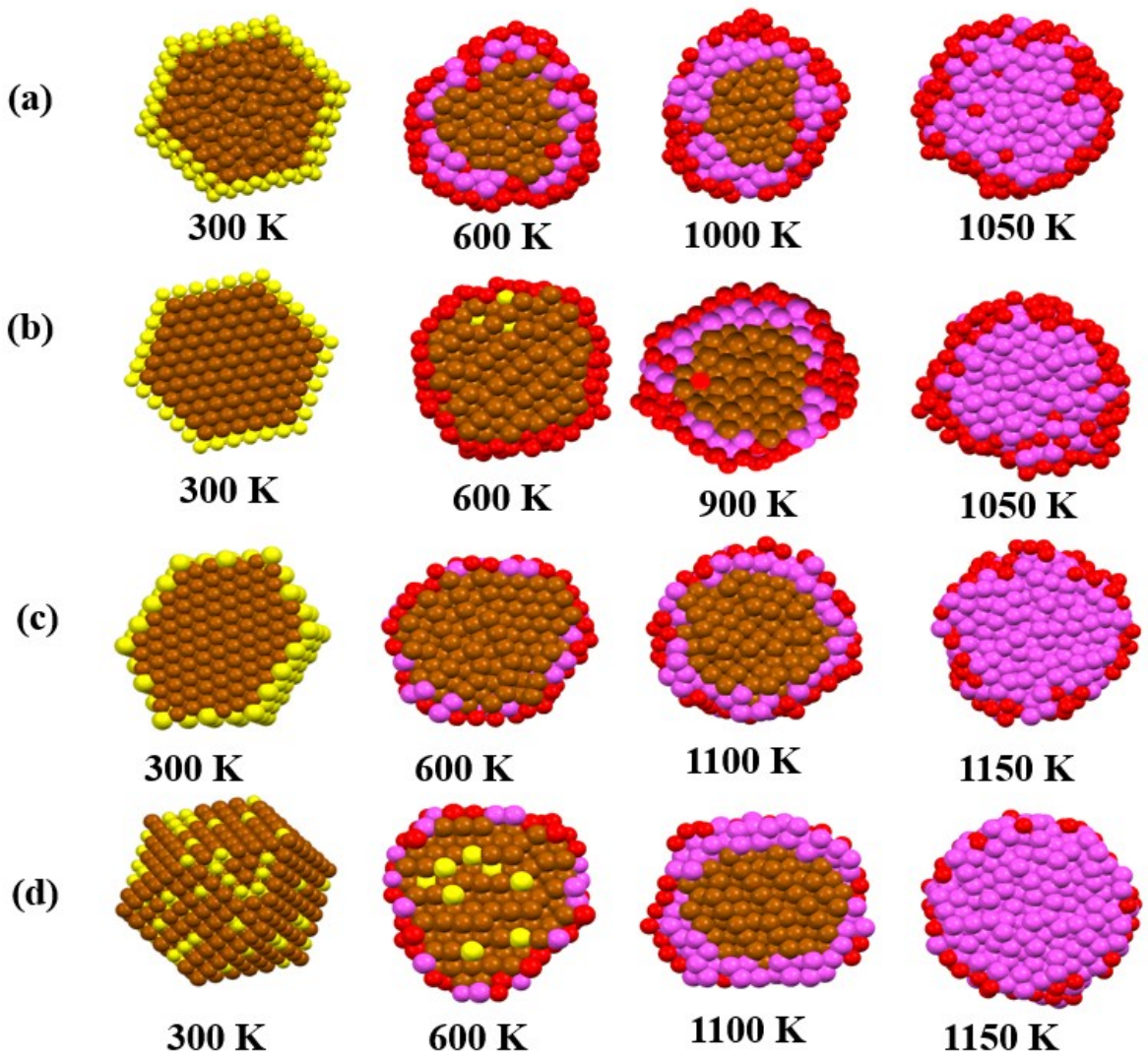

Figure S5. Snapshots of cross sections of $Au_{0.23}$ $Fe_{0.77}$ bimetallic nanoclustersincluding (a) Fe@Au NPs with amorphous-core (a), fcc-core (b), bcccore (c), and Au-Fe nanoalloy (d)during the heating process. Coloring denotes type of atom: yellow, solid Au atom; brown, solid Fe atom; red, liquid Au atom; and pink, liquid Fe atom.

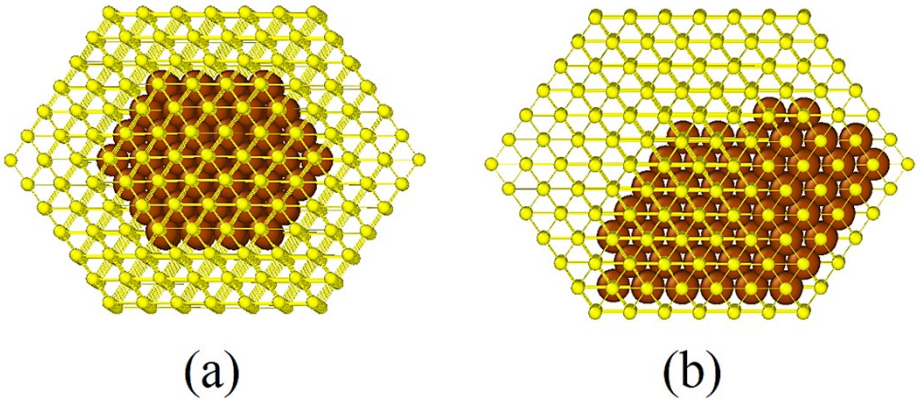

Figure S6. (a) Au-rich $Fe_{0.23}@Au_{0.77}$ with centered core, and (b) Au-rich $Fe_{0.23}@Au_{0.77}$ with off-centered core.

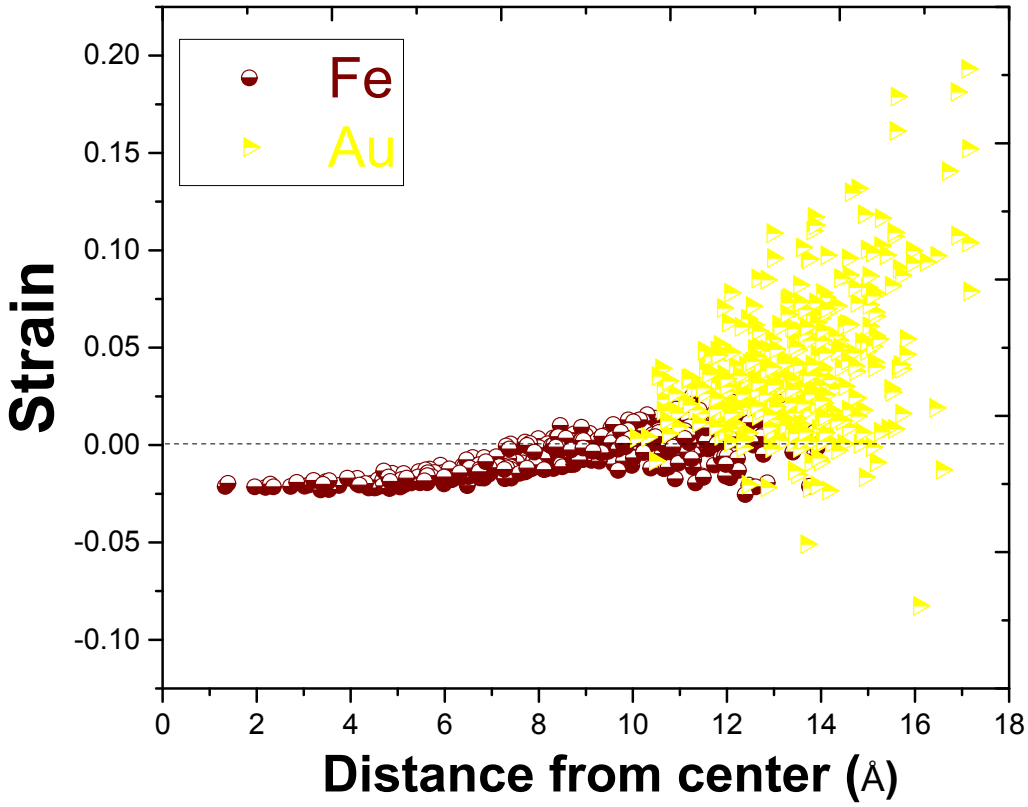

Figure S7. Strain plots for $Au_{0.23}Fe_{0.77}$ nanocluster at 400 K.

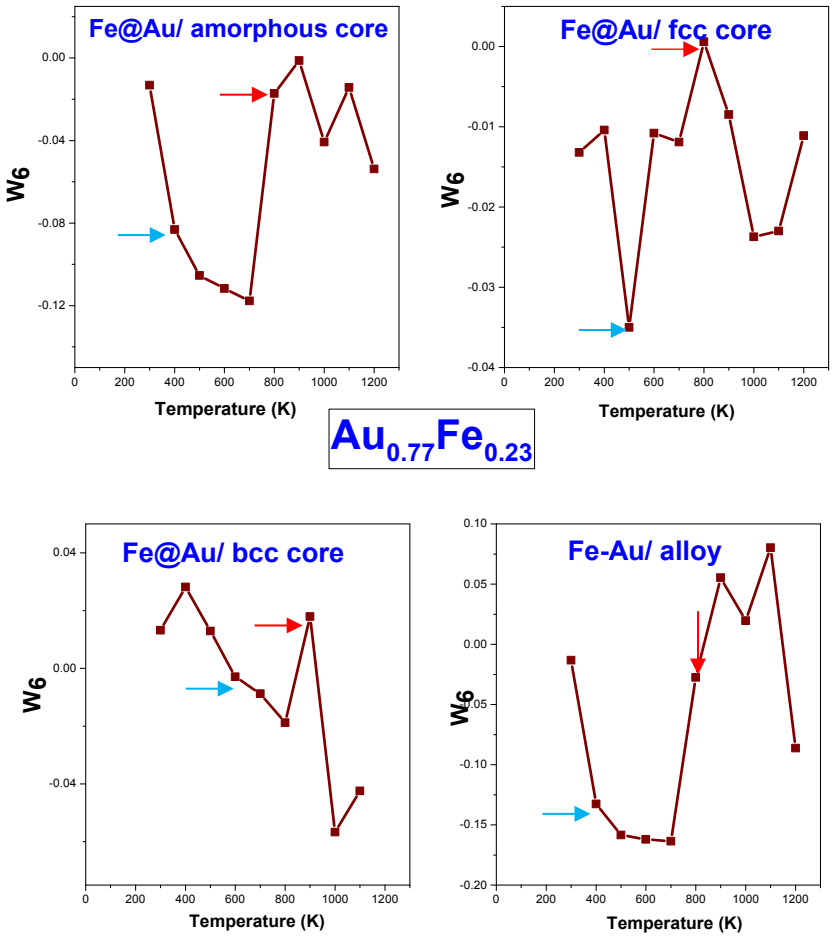

Figure S8. The Winger parameter (W_6) at different temperatures for four types of $Au_{0.77}Fe_{0.23}$ bimetallic nanoclusters.

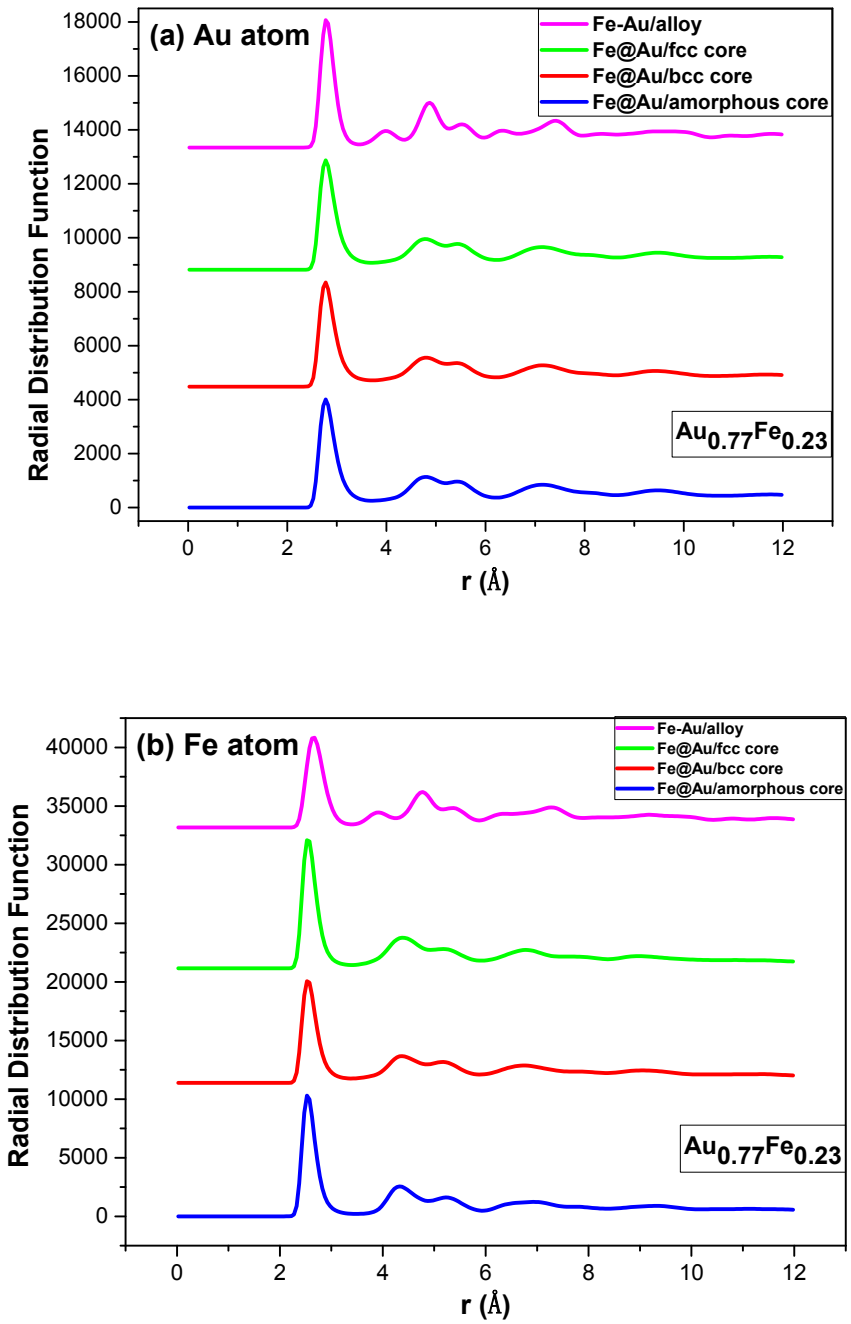

Figure S9. Radial distribution function of (a) Au-Au and (b) Fe-Fepairs in $Au_{0.77}Fe_{0.23}$ bimetallic nanoclusters at 400 K.

Geometry	$\hat{W}_6$
fcc	-0.013161
hcp	-0.012442
bcc	0.013161
icos	-0.169754
sc	0.013161
Liquid	0

Table S1: Wigner values for six typical structures (face-centered-cubic (fcc), hexagonal-close-packed (hcp), body-centered-cubic (bcc), icosahedral clusters (icos), simple-cubic (sc), and liquid structure).